

Electrically assisting crystal growth of blue phase liquid crystals

Michael Chen, Yi-Hsin Lin,* Hung-Shan Chen, and Hung-Yuan Chen

Department of Photonics, National Chiao Tung University, Hsinchu 30010, Taiwan

yilin@mail.nctu.edu.tw

<http://web.it.nctu.edu.tw/~yilin>

Abstract: We proposed an electrically assisting crystal growth of blue phase liquid crystals (BP-LCs) to generate uniform crystal orientation of BP-LCs. With an applied electric field, a phase transition from BP-LCs to focal conic state and homeotropic state occurs. As the electric field is removed, the crystal orientation of [220] quickly dominates the crystal growth process and other crystal orientations grow less at the same time. The BP-LCs with a single crystal orientation can be achieved with multiple cycles of the electrical treatment. We also provide a possible mechanism of crystal growth with electrical treatment which is applicable for both BP-LCs and PSBP-LCs. In addition, we conclude that the hysteresis effect is mainly affected by the domain size of PSBP-LCs rather than uniformity of crystal orientation. This study helps further understanding of the origin of hysteresis effect in PSBP-LCs which is important for development of many BP-LCs based photonic devices, such as micro lenses, displays, and lasers.

©2014 Optical Society of America

OCIS codes: (230.3720) Liquid-crystal devices; (160.3710) Liquid crystals.

References and links

1. A. Hauser, M. Thieme, A. Saupe, G. Heppke, and D. Krueker, "Surface-imaging of frozen blue phases in a discotic liquid crystal with atomic force microscopy," *J. Mater. Chem.* **7**(11), 2223–2229 (1997).
2. H. S. Kitzerow, "Blue phases come of age: a review," *Proc. SPIE* **7232**, 723205, 723205-14 (2009).
3. E. Demikhov, H. Stegemeyer, and V. Tsukruk, "Pretransitional phenomena and pinning in liquid-crystalline blue phases," *Phys. Rev. A* **46**(8), 4879–4887 (1992).
4. D. C. Wright and N. D. Mermin, "Crystalline liquids: the blue phases," *Rev. Mod. Phys.* **61**(2), 385–432 (1989).
5. P. P. Crooker, "The blue phases. A review of experiments," *Liq. Cryst.* **5**(3), 751–775 (1989).
6. Y. H. Lin, H. S. Chen, H. C. Lin, Y. S. Tsou, H. K. Hsu, and W. Y. Li, "Polarizer-free and fast response microlens arrays using polymer-stabilized blue phase liquid crystals," *Appl. Phys. Lett.* **96**(11), 113505 (2010).
7. Y. H. Lin, H. S. Chen, and T. H. Chiang, "A reflective polarizer-free electro-optical display using dye-doped polymer-stabilized blue phase liquid crystals," *J. Soc. Inf. Disp.* **20**(6), 333–336 (2012).
8. H. J. Coles and M. N. Pivnenko, "Liquid crystal 'blue phases' with a wide temperature range," *Nature* **436**(7053), 997–1000 (2005).
9. M. Kimura, N. Nagumo, T. N. Oo, N. Endo, H. Kikuchi, and T. Akahane, "Single-substrate polymer-stabilized blue phase liquid crystal display," *Opt. Mater. Express* **3**(12), 2086–2095 (2013).
10. W. Cao, A. Muñoz, P. Palfy-Muhoray, and B. Taheri, "Lasing in a three-dimensional photonic crystal of the liquid crystal blue phase II," *Nat. Mater.* **1**(2), 111–113 (2002).
11. Y. H. Chen, C. T. Wang, C. P. Yu, and T. H. Lin, "Polarization independent Fabry-Pérot filter based on polymer-stabilized blue phase liquid crystals with fast response time," *Opt. Express* **19**(25), 25441–25446 (2011).
12. G. Zhu, B. Y. Wei, L. Y. Shi, X. W. Lin, W. Hu, Z. D. Huang, and Y. Q. Lu, "A fast response variable optical attenuator based on blue phase liquid crystal," *Opt. Express* **21**(5), 5332–5337 (2013).
13. H. Kikuchi, M. Yokota, Y. Hisakado, H. Yang, and T. Kajiyama, "Polymer-stabilized liquid crystal blue phases," *Nat. Mater.* **1**(1), 64–68 (2002).
14. F. Castles, F. V. Day, S. M. Morris, D.-H. Ko, D. J. Gardiner, M. M. Qasim, S. Nosheen, P. J. W. Hands, S. S. Choi, R. H. Friend, and H. J. Coles, "Blue-phase templated fabrication of three-dimensional nanostructures for photonic applications," *Nat. Mater.* **11**(7), 599–603 (2012).
15. K. M. Chen, S. Gauza, H. Xianyu, and S. T. Wu, "Hysteresis effects in blue-phase liquid crystals," *J. Disp. Technol.* **6**(8), 318–322 (2010).
16. L. Rao, J. Yan, S. T. Wu, Y. C. Lai, Y. H. Chiu, H. Y. Chen, C. C. Liang, C. M. Wu, P. J. Hsieh, S. H. Liu, and K. L. Cheng, "Critical field for a hysteresis-free BPLC device," *J. Disp. Technol.* **7**(12), 627–629 (2011).

17. C. Y. Fan, C. T. Wang, T. H. Lin, F. C. Yu, T. H. Huang, C. Y. Liu, and N. Sugiura, "Hysteresis and residual birefringence free polymer-stabilized blue phase liquid crystal," *SID Int. Symp. Digest Tech. Papers* **42**, 213–215 (2011).
18. L. Wang, W. He, Q. Wang, M. Yu, X. Xiao, Y. Zhang, M. Ellahi, D. Zhao, H. Yang, and L. Guo, "Polymer-stabilized nanoparticle-enriched blue phase liquid crystals," *J. Mater. Chem. C* **1**(40), 6526–6531 (2013).
19. Y. F. Lan, C. Y. Tsai, J. K. Lu, and N. Sugiura, "Mechanism of hysteresis in polymer-network stabilized blue phase liquid crystal," *Polymer (Guildf.)* **54**(7), 1876–1879 (2013).
20. A. Yoshizawa, M. Kamiyama, and T. Hirose, "Amorphous blue phase III exhibiting submillisecond response and hysteresis-free switching at room temperature," *Appl. Phys. Express* **4**(10), 101701 (2011).
21. H. S. Chen, Y. H. Lin, C. H. Wu, M. Chen, and H. K. Hsu, "Hysteresis-free polymer-stabilized blue phase liquid crystals using thermal recycles," *Opt. Mater. Express* **2**(8), 1149–1155 (2012).
22. Y. Chen and S. T. Wu, "Electric field-induced monodomain blue phase liquid crystals," *Appl. Phys. Lett.* **102**(17), 171110 (2013).
23. J. Yan, Y. Chen, D. Xu, and S. T. Wu, "Angular dependent reflections of a monodomain blue phase liquid crystal," *J. Appl. Phys.* **114**(11), 113106 (2013).

1. Introduction

Blue phase liquid crystals (BP-LCs) usually exists between a cholesteric state and an isotropic state, which possesses a structure of double twist cylinders and then forms as three-dimensional photonic crystals. Based on different lattice structures, BP-LCs can be categorized as: body center cubic structure of BPI, simple cubic structure of BPII and amorphous structure of BPIII [1–5]. BP-LCs is an ideal electro-optical materials for photonic devices due to advantages of optical isotropy, field-induced Kerr effect, natural Bragg's reflection, sub-millisecond response time and free of alignment layers. Lots of photonic applications have been demonstrated, including microlens arrays, a dye-doped electro-optical switch displays, three dimensional mirror-less lasers, Fabry Perot filters, and variable optical attenuators [6–12]. Typically, BP-LCs exists in a narrow temperature range which can be extended to around 60°C using polymer networks to stabilize structure of BP-LCs [13]. Moreover, BP-LCs with a templated method was demonstrated and the temperature range was further extended from –125°C to 125°C [14]. However, hysteresis effect in polymer-stabilized blue phase LCs (PSBP-LCs) still hinders the development of BP-LCs based devices [7, 15]. Therefore, many researchers proposed methods to reduce hysteresis, such as an operation of low driving voltage [16], an adjustment of polymer networks [17], a method of nano-particle stabilization [18], and frequency switching method [19]. In addition, it was found that polymer-stabilized BPIII was hysteresis-free in spite of a relatively narrow temperature range as well as high operational voltage [20]. In 2012, we also demonstrated a hysteresis-free PSBP-LCs by thermally manipulating the competition between a homogeneous nucleation and a heterogeneous nucleation during the crystal growth of PSBP-LCs [21]. From the experimental results, the PSBP-LCs with a large domain size and a uniform crystal orientation exhibits no hysteresis. However, whether the domain size or crystal orientation is the key factor to affect hysteresis is still unclear. In 2013, Y. Chen et. al. and J. Yan et. al. achieved a monodomain PSBP-LCs by applying a single electric field and they also demonstrated an application for a reflective display [22,23]. However, the crystal growth of the blue phase texture and phase transition process under the electric field were not discussed in detail. In this paper, we demonstrate an electrically assisting crystal growth of blue phase liquid crystals to achieve BP-LCs with single crystal orientation and propose a mechanism of how electrical field assists crystal growth of BP-LCs. The BP-LCs turned into focal conic textures and homeotropic states when we applied an electric field, and a more uniform BP-LCs re-grew as the electric field was removed. After the sample was treated with several cycles of voltage, the BP-LCs appeared in a uniform crystal orientation of [220] while the domain size was hardly changed. Then we prepared a PSBP-LCs sample with electrical treatment and observed its electro-optical effect. Finally, we discuss and conclude the main reasons for the origin of hysteresis effect based on the experimental results.

2. Sample preparation and experiments

The sample of BPLC is prepared in the follows process. We mixed a positive nematic host LC ($\Delta n = 0.142$) with a chiral molecules CB15 (Merck) at 61.3:38.7 wt% ratios. The blue

phase of mixtures appeared between 37.1 °C and 41.1°C. The mixture at isotropic state (~50°C) was filled into an empty LC cell consisting of two ITO glass substrates without any alignment layers and the cell gap was 7.5 μm. The crystal growth process with an applied voltage of 13V_{rms} was observed at the temperature 40.3°C. As to the sample of polymer-stabilized blue phase liquid crystals (PSBP-LCs), we mixed our BP-LCs with two UV-curable monomers, EHA (2-Ethylhexyl, Fluka) and RM257 (Merck), and photo-initiator DMPAP (Aldrich) at 92.25: 3.35: 3.45: 0.95 wt% ratios. The crystal growth process for PSBP-LCs with an applied voltage of 16V_{rms} was conducted at the temperature 29.7°C. After the electrical treatment, the cell was then exposed by UV light with UV intensity of ~1.5mW/cm² for 60 minute for photo-polymerization. The PSBP-LCs exists in blue phase within a temperature range from 20°C to 42°C.

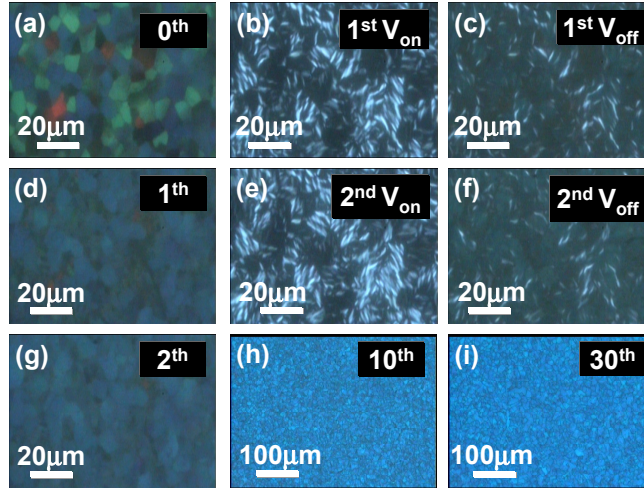


Fig. 1. Morphologies of BPLC sample under a reflective polarizing microscope at 40.3°C (a) without an applied voltage. (b) The morphology during the first applied voltage. (c) The morphology after the voltage turns off. Blue crystal grows. (d) The morphology after (c) for 5 sec. (e) The morphology during the second applied voltage. (f) The morphology after turning off the second applied voltage. (g) The morphology after (f) for 5 sec. (h) and (i) are the morphologies of BP-LC after the 10th and the 30th cycles of applied voltages, respectively. $V = 13V_{rms}$, and $f = 1\text{kHz}$.

In order to investigate the crystal growth process under an applied electric field, we observed the morphologies of BP-LCs at 40.3°C under a reflective polarizing optical microscopy (POM) (Leica, DM-2500D) and recorded the images, as shown in Fig. 1. In Fig. 1(a), the mixture was first cooled down from the isotropic state to 40.3°C and exhibited morphology of BP-LCs. The BP-LCs appeared in blue, green, and red which means different crystal orientations due to a homogeneous nucleation and a heterogeneous nucleation occurred simultaneously [20]. When we applied an alternating current (AC) voltage of 13V_{rms} with a frequency of 1kHz to the sample for 1sec, phase transition of BP-LCs occurred as shown in Fig. 1(b). Small white stripes in Fig. 1(b) were originated from light scattering due to focal conic textures while the dark regions under crossed polarizers were composed of homeotropic states which means LC directors orient perpendicular to the glass substrate locally. The homeotropic states can further be proved by Kossel diagram in the next paragraph. Figure 1(c) is the morphology taken as soon as we turned off the applied voltage. Most of the focal conic states turned into BP-LCs with blue Bragg's reflection when the external electric field was removed. Moreover, the dark regions in Fig. 1(c) were changed gradually to BP-LCs with different crystal orientations (red, green and blue domains). After we removed the applied voltage for ~5sec, the whole observed area turned into BP-LCs, as shown in Fig. 1(d). Compared to Fig. 1(a), the crystal orientations of BP-LCs in Fig. 1(d) were more uniform in blue where red and green crystal orientations decreased. In Fig. 1(e),

when the applied voltage turned on again, more regions turned into focal conic states which showed white scattered light and the dark regions were less than those in Fig. 1(b). Therefore, more BP-LCs with blue crystal orientation appeared as we turned off the applied voltage again, as depicted in Fig. 1(f). Figure 1(g) shows that the red and green domains almost disappeared and the crystal orientation of BP-LCs was more uniform with blue Bragg's reflection after the second crystal nucleation process. We repeated the electrical treatment, the process of applying voltage on and off for many cycles. Figures 1(h), and 1(i) shows the morphologies of BP-LCs after we applied the voltage for 10 and 30 times, respectively. When the voltage was applied for over 10 times, the BP-LCs appeared in single crystal orientation, which resulted in uniform blue Bragg's reflection. Moreover, the domain size of BP-LCs was not obviously enlarged with the cycles of electrical treatment as it were through the thermal treatment [21]. From the observation of morphologies, we found that the blue crystal orientation increases while the other crystal orientations decrease when we increase the cycles of electrical treatment. Finally, BP-LCs with single crystal orientation can be achieved by applying an external voltage for several times.

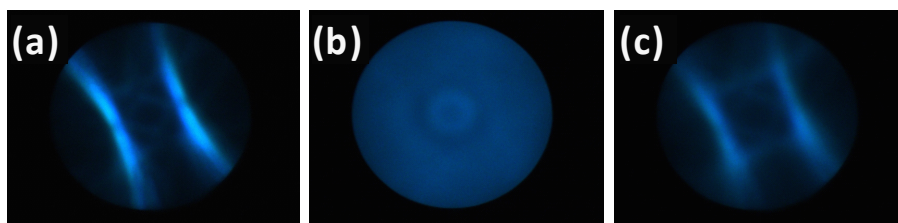


Fig. 2. Kossel diagrams of the blue area of the BP-LC sample (a) before, (b) during, and (c) after applying a voltage of $13V_{rms}$. Before taking photos of Kossel diagrams, the BP-LC sample experiences electrical treatment 200 times. $\lambda = 510nm$

In order to further investigate the phase transition process under an applied electric field, we observed the corresponding Kossel diagrams of BP-LCs with a uniform crystal orientation whose domain size was $\sim 100\mu m$ after 200 cycles of electrical treatment. Then we observed the Kossel diagrams of BP-LCs during one more cycle of electrical treatment. Figure 2(a) shows the Kossel diagram before we applied a voltage of $13V_{rms}$. At this moment, the sample was at the state of BP-LCs due to the clear Kossel pattern. While we turned on the voltage, the observed image is shown as Fig. 2(b). The disappearance of Kossel lines states that BP-LCs experiences a phase transition and the double twist structure of BP-LCs vanishes. Besides, the brightness of whole observation region in Fig. 2(b) increased because of light scattering resulting from the focal conic states or the white stripes in Figs. 1(b) and 1(e). Moreover, a weak ring pattern in the center of Fig. 2(b) was most likely contributed by the conoscopic profile of homeotropic state. Therefore, the dark areas in Figs. 1(b) and 1(e) are liquid crystals aligned with electric fields in the form of a homeotropic state rather than an isotropic state. After the applied voltage was removed, the sample turned back to the state of BP-LCs again, and the Kossel diagram was recorded as Fig. 2(c). Although the crystal orientation remained the same compared to Fig. 2(a), the weaker diffraction signal and additional Kossel lines point out that the grain boundaries increased after the electrical treatment. This explains the reason why the domain size of BP-LCs cannot increase efficiently with the increasing cycles of applied voltage.

To explain the mechanism of the crystal growth under electric fields, we also have to identify the crystal orientations. The Kossel lines in Fig. 2(a) shows in the form of hyperbola. This indicates that blue crystal orientations in Fig. 1(a) belong to BPII with simple cubic structure, and the crystal orientation is parallel to $[110]$ (e.g. $[110]$, $[220]$ etc) [1]. Moreover, the minimum transmittance appears at $\lambda = 475nm$ (data are not shown here), which represents the wavelength of Bragg reflection. The relation between the wavelength of Bragg reflection and the crystal orientation can be expressed as [1]:

$$\lambda = \frac{2 \times n \times a \times \cos \theta}{\sqrt{h^2 + k^2 + l^2}}, \quad (1)$$

where n is the average refractive index of the BP-LCs, “ a ” is the lattice constant of the BP-LC, θ is the angle of Bragg reflection, and (h,k,l) are the Miller indices. Assume the refractive index and the lattice constant for different crystal orientations are identical due to the same BP-LC mixture. Then the most probable crystal orientation of the blue domains is $[220]$, which can allow two shorter Bragg reflection wavelengths in visible range corresponding to red and green crystal orientations. Therefore, based on Eq. (1), the crystal orientation is $[211]$ and the peak reflection wavelength is 549nm for green domains while the crystal orientation is $[200]$ with Bragg reflection at $\lambda = 672\text{nm}$ for the red domains.

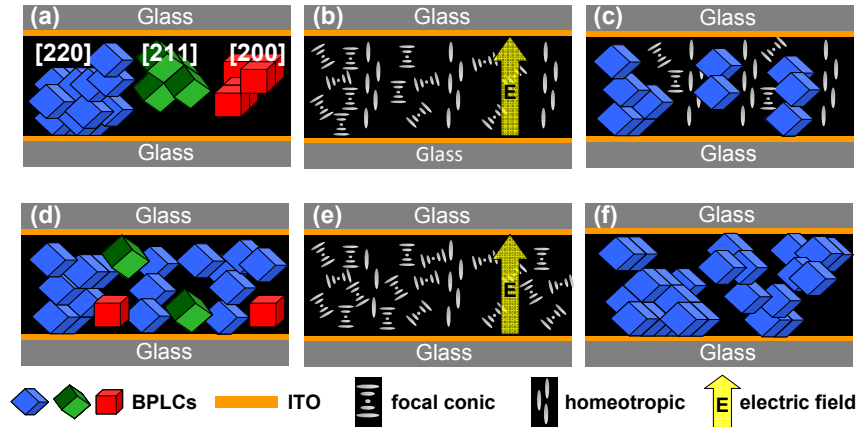


Fig. 3. A possible mechanism of nucleation process of BP-LC under the electrical treatment. (a) BP-LCs have crystal orientations of $[220]$, $[211]$ and $[200]$, and the isotropic phase is represented by the rest of region (black part). (b) A phase transition to the focal conic state and the homeotropic state occur as an electric field is applied. (c) Most of the focal conic state turns into $[220]$ crystal when the electric field is removed. The rest of the region grows randomly with red, green, and blue crystals until the whole mixture turns into BP-LCs, as depicted in (d). (e) More focal conic state appears when the electric field is applied again. (f) BP-LCs turn out the single crystal orientation of $[220]$ after several cycles of processes (c), (d), and (e).

Based on the experimental results, a possible mechanism of a crystal growth of BP-LCs under electrical treatments is proposed in the illustrations of Figs. 3(a)-3(e). First, the mixture is cooled down from isotropic phase until it completely turns into BP-LCs. In Fig. 3(a), the crystal orientations of BP-LCs appear randomly resulting from both of homogeneous nucleation and heterogeneous nucleation [21]. Blue, green, and red cubes in Fig. 3(a) stand for BP-LCs with crystal orientations of $[220]$, $[211]$ and $[200]$, respectively. When an electric field is applied in Fig. 3(b), such an electric field results in a phase transition of most of BP-LCs to focal conic state; meanwhile, liquid crystal molecules in the rest parts are aligned by the electric field, so-called a homeotropic state, as depicted in Fig. 3(b). When the electric field is removed, most of focal conic state goes back to BP-LCs with a uniform crystal orientation of $[220]$ in Fig. 3(c). Then those homeotropic state areas in Fig. 3(c) gradually turn into BP-LCs with random crystal orientations depicted in Fig. 3(d). Blue crystals of $[220]$ increase while green crystals of $[211]$ and red crystals of $[200]$ decrease in comparison with Fig. 3(a). When the electric field is applied again, more BP-LCs in Fig. 3(e) turn into focal conic state and less portion of BP-LCs turn into homeotropic state in comparison to Fig. 3(b). As a result, more BP-LCs with a $[220]$ crystal orientation instantly grow again from focal conic state as the electric field is removed again. Blue crystals dominate the whole region and other crystals almost vanish. After repeating the processes of applying an electrical field in

Figs. 3(c)-3(e), red and green crystals can be totally eliminated and the BP-LCs finally has a single crystal orientation of [220], as shown in Fig. 3(f). Moreover, when the electric field is applied, BP-LCs turns into either focal conic state or homeotropic state without grain boundaries. However, new grain boundaries appear when the electric field is removed. This is the reason why the domain size of BP-LCs has no significant change as the cycle of electrical treatment increases. Blue crystals increase as the others decrease after each cycle of electrical treatment. Therefore, we can easily achieve a BP-LCs with single crystal orientation by periodically manipulating the external electric field several times. After the BP-LCs appears in uniform crystal orientation, we can use monomers and photo-polymerization process to freeze the morphology BP-LCs which is so-called PSBP-LCs for practical applications.

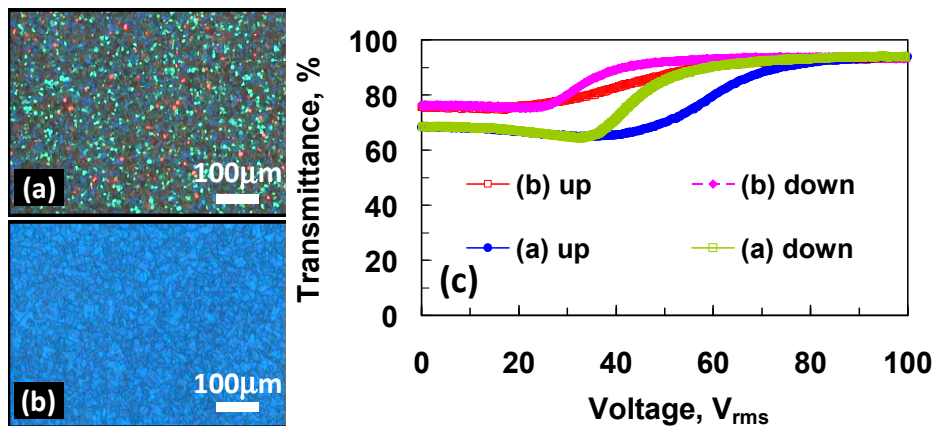


Fig. 4. The morphologies of PSBP-LCs (a) without any treatment and (b) with applying an electrical field 10 times. (c) The voltage-dependent transmittance of PSBP-LCs of samples in (a) and (b) with an increasing voltage (up) and a decreasing voltage (down).

In order to measure the electro-optical properties, we prepared two samples of PSBP-LCs with and without electrical treatments. The reason why we adopted monomer into BP-LCs (i.e. PSBP-LCs) is to fix the morphologies of the BPLC after electrical treatment and also prevent the generation of focal conic states which could affect the measured electro-optical properties of the samples. Two samples were prepared under same condition except the electrical treatment. The morphologies are shown in Figs. 4(a) and 4(b). In Fig. 4(a), the morphology of PSBP-LCs without electrical treatment showed different crystal orientations [220], [211] and [200] and the domain size is small $\sim 10\mu\text{m}$. In Fig. 4(b), the morphology of PSBP-LCs with 10 cycles of electrical treatments shows single crystal orientation [220]. The domain size of PSBP-LCs with electrical treatment was around $\sim 15\mu\text{m}$. The experimental setup for measuring the electro-optical properties of PSBP-LC samples is introduced as follows. A He-Ne laser (Melles Griot, Model 05-LGR-173, $\lambda = 543\text{ nm}$) was normally impinged on the samples and the transmitted optical intensity under different applied voltages was detected by a photo detector placed 25cm away behind the samples. The optical intensity was normalized with the transmission of an empty cell. The measured voltage-dependent transmittance of the PSBP-LC samples with an increase of voltage and a decrease of voltage are shown in Fig. 4(c). At $V = 0$, PSBP-LCs without electrical treatment shows lower transmittance compared to PSBP-LCs with electrical treatment because different orientations of crystals and small domain size in Fig. 4(a) result in more Bragg's reflection and light scattering. PSBP-LCs with electrical treatment shows slightly lower hysteresis than the one without electrical treatment. In our previous discussion of hysteresis of PSBP-LCs, we have reported that the hysteresis of PSBP-LCs can be eliminated by thermally manipulating nucleation of the crystal growth of BPLC [21]. The domain size was enlarged to over $60\mu\text{m}$ and the crystal orientation of PSBP-LCs was more uniform than PSBP-LCs in Fig. 4(a) after 10 cycles of thermal treatment. In the previous results of thermal treatment, we conclude the hysteresis could be reduced by large domain size and uniform crystal orientations [21].

However, the experimental results in this paper indicate that hysteresis effect has nothing to do with the uniformity of the crystal orientation rather than have a strong relation with the domain size of PSBP-LCs. When the domain size is relatively small, strong anchoring energy between BP-LCs and polymer network is generated from the large number of grain boundaries. As a result, hysteresis is enhanced [19]. As the domain size is enlarged, the number of grain boundaries of PSBP-LCs decreases resulting in the reduction of hysteresis effect. The measured switching times are 2.67ms and 2.98ms for PSBP-LCs with and without the electrical treatment, respectively. The Kerr constant of both samples are $\sim 7.5 \times 10^{-10} \text{ m/V}^2$ at the temperature of 25°C. Therefore, the response time and the Kerr constant of PSBP-LCs remain similar no matter the sample has the electrical treatment or not. For many applications that prefer uniform crystal orientation without hysteresis, we may combine the electrical and thermal recycling processes to realize a hysteresis-free PSBP-LCs with single crystal orientation.

3. Conclusion

We electrically manipulate the crystal growth of BP-LCs with an applied electric field and discuss the mechanism. When an external voltage is applied on the sample, BP-LCs turns into focal conic state and homeotropic state, and the area of focal conic state increases with the cycles of applied voltage. A preferred crystal orientation of [220] grows rapidly from focal conic state and restricts the growth of other crystal orientations as the applied voltage is turned off. Therefore, BP-LCs with single crystal orientation can be achieved while the domain size remains similar. Comparing the electro-optical properties between PSBP-LCs with different morphologies, it turns out that hysteresis is less affected by the uniformity of crystal orientation. Hysteresis effect disappears only when the domain size of PSBP-LCs is sufficiently enlarged where the grain boundaries are reduced [21]. A method of further elimination of the grain boundaries and how to realize a BP-LCs with extremely large domain size would be interesting and make BP-LCs more suitable for practical applications. We believe this study can facilitate the development of PSBP-LC based photonic devices.

Acknowledgments

The authors would like to thank Prof. Ru-Pin Pan (National Chiao Tung University) for the Kossel Diagrams. This research was supported partially by Innolux Corp. and partially by the National Science Council (NSC) in Taiwan under the contract no. NSC 101-2112-M-009-011-MY3.